Optical molecular imaging of lymph nodes using a targeted vascular contrast agent

Kai Licha
Niels Debus
Sonja Emig-Vollmer
Birte Hofmann
Michael Hasbach
Dietger Stibenz
Sabine Sydow
Michael Schirner
Schering AG
Research Laboratories
D-13342 Berlin, Germany
E-mail: kai.licha@schering.de

Bernd Ebert
Diethard Petzelt
Physikalisch-Technische Bundesanstalt
Abbestr. 2-12
D-10587 Berlin, Germany

Christoph Bührer
Berlin University Medical Center
Deptartment of Neonatology
Charité-Campus Virchow-Klinikum
D-13353 Berlin, Germany
and
University Children's Hospital
CH-4005 Basel, Switzerland

Wolfhard Semmler
Deutsches Krebsforschungszentrum
Im Neuenheimer Feld 280
D-69120 Heidelberg, Germany

Rudolf Tauber
Berlin University Medical Center
Institute of Clinical Chemistry and Pathological Biochemistry
Charité Campus Benjamin Franklin
D-12200 Berlin, Germany

Abstract. We develop a highly specific antibody-dye conjugate for optical imaging of peripheral lymph nodes. The contrast agent consists of the monoclonal antibody recognizing endothelial ligands for the lymphocyte homing receptor L-selectin, MECA-79, and a near-infrared (near-IR) fluorescent indotricarbocyanine dye. The targeting and biodistribution behavior of MECA-79 is studied after radioiodination and intravenous injection into mice demonstrating specific uptake in lymph nodes and accumulation in high endothelial venules (HEV). After conjugation of MECA-79 with indotricarbocyanine dye, the fluorescence imaging properties of the MECA-79 dye conjugate are examined by intravenous injection in nude mice and laser-induced fluorescence whole-body imaging *in vivo*. The MECA-79 antibody-dye conjugate accumulates in peripheral lymph nodes, whereas an isotype antibody-dye conjugate does not. Specific lymph node near-IR fluorescent signals become detectable within minutes after injection, and stable imaging persists for more than 24 h. The results demonstrate that vascular targeting of endothelial expression of glyocproteins is feasible to visualize the accumulation of near-IR fluorescent MECA-79 in lymph nodes, making this technology potentially useful to characterize processes of inflammation. [DOI: 10.1117/1.2007967]

Keywords: optical imaging; lymph nodes; vascular targeting; near-IR fluorescent dye conjugates.

Paper 05060 SSR received Mar. 4, 2005; revised manuscript received Apr. 29, 2005; accepted for publication May 3, 2005; published online Aug. 10, 2005.

1 Introduction

Biomedical optical imaging is an emerging technology that has created promising opportunities for biomedical research and medical care in the past few years.[1–3] Major driving forces have been both the instrumental and physical advances in the areas of lasers, detection techniques, and image reconstruction,[4–7] and chemical/biotechnological progress in the design of novel fluorescent reporter systems.[2,3,8,9] The availability of specific fluorescent compounds reporting molecular characteristics of early diseases *in vivo* is crucial for the application of optical techniques as a noninvasive, easy-to-use molecular imaging modality. A host of different fluorescent organic dye entities and inorganic reporter systems have demonstrated versatile utility as biocompatible imaging probes, including targeted small molecule and peptide conjugates,[10–13] labeled antibodies and other proteins,[14–16] and enzyme-activatable carrier systems.[8,17,18]

The ability to detect metastatically involved lymph nodes contributes decisively to the long-term success of cancer surgery. Optical methods are predestined for the imaging of superficial tissues areas. Several publications describe the use of fluorescent markers, such as organic dyes[19,20] or semiconduc-

Address all correspondence to Kai Licha, Medicinal Chemistry, Schering AG, Muellerstr. 178, Berlin, 13342 Germany. Tel: +49–30–4681–7703. Fax: +49–30–4689–7703. E-mail: kai.licha@schering.de

1083-3668/2005/10(4)/041205/6/$22.00 © 2005 SPIE

tor quantum dots,[21–23] directed toward the improved identification and mapping of lymph nodes, in particular sentinel lymph nodes during surgery, beyond the established "blue dye" procedure.[24] These approaches, however, only work properly with contrast agents locally applied in the vicinity of the respective target organs and are not directed toward the characterization of disease-specific molecular events.[25,26] Particularly, the imaging of molecular expression of inflammatory processes has not been the underlying rationale of previous work.

The entry of leukocytes into the lymphatic system or into inflamed tissue is mediated by cell adhesion events involving leukocytes and endothelial cells located at the wall of blood vessels. The constitutive recirculation of lymphocytes into peripheral lymph nodes—a process known as homing—requires the interaction between L-selectin, an adhesion molecule expressed exclusively on leukocytes, and glycoproteins found on the luminal side of specialized high endothelial venules (HEV) in lymph nodes.[27–31] These glycoproteins are recognized by the immunoglobulin M (IgM) monoclonal antibody MECA-79.[27,31,32] The contrast agent described here employs this monoclonal antibody coupled to a near-IR fluorescent cyanine dye. As the target of the antibody is found on the luminal side of the endothelial lining of lymph node blood vessels, it can easily reach its target without penetrating the surrounding tissue. Thus, the underlying targeting principle omits the need to design agents combining target affinity with the aspect of tissue penetration, which is often a limiting issue for the use of antibodies. The diagnostic potential of MECA-79 has been studied for target-specific ultrasound imaging of lymph nodes using air-filled microparticles,[33] which are too big in diameter ($\sim$1 μm) to extravasate from the blood vessel into interstitial compartments.

We describe the suitability of the MECA-79 antibody as a vehicle for optical molecular imaging by studying the targeting and biodistrubution properties and the feasibility to detect vascular glycoprotein expression of lymph nodes with fluorescence imaging.

2 Experimental

2.1 *Materials and Preparation*

The near-IR fluorescent dye used in this study was bis-1,1′-(4-sulfobutyl)-indotricarbocyanine-5-carboxylic acid N-hydroxysuccinimidyl ester, sodium salt. The synthesis of this compound was described previously in detail.[34,35] MECA-79 and control antibody R4-22 (both 0.5 mg/mL in 50-mM TRIS buffer, pH 8.0, +500-mM NaCl) were purchased from Pharmingen International (Heidelberg, Germany). Both antibodies are IgM-type antibodies of approximately 1000-kDa molecular weight. For labeling with near-IR cyanine dyes, both antibodies were transferred into 50-mM carbonate buffer and concentrated to 0.5 mg/mL (ultracentrifugation). Labeling of antibodies was achieved as follows: 1-mg antibody in 1-ml 50-mM carbonate buffer was incubated with a 30-fold molar excess of dye (freshly prepared stock solution 1.8 mg/mL dye in distilled water) for 24 h at room temperature. Unreacted dye was removed by gel filtration (NAP10 column, elution with phosphate-buffered saline, pH 7.4). Radiolabeling of MECA-79 was performed with chloramin-T/^{123}I-sodium iodide according to standard procedures.[36] Briefly, 50-μg antibody (0.5 mg/mL) was treated with 2-μL $Na^{125}I$ or $Na^{125}I$ (200 μCi) and 30-μL chloramin T (8 mg/mL) for 2 min. at room temperature, followed by 60-μL $Na_2S_2O_5$ (8 mg/mL) and 0.5-mL cold NaI (2 mg/mL) to stop the reaction. Purification was achieved by filtration on PD10 columns (Pharmacia Biotech) using phosphate-buffered saline (PBS). Immunohistochemistry using biotinylated MECA-79 was conducted as described in Ref. 33.

2.2 *Photophysical Characterization*

Absorption spectra were measured using a Lambda-2 photometer (Perkin-Elmer GmbH, Überlingen, Germany). Dye-to-protein ratios were calculated from the absorption spectra as described in Ref. 35, assuming an OD of 1.4 for a concentration of 1 mg/ml of antibodies. Fluorescence emission spectra of 2-μmol/I aqueous dye solutions were recorded in the front-face mode using a SPEX Fluorolog fluorometer (Instruments S.A. GmbH, Grasbrunn, Germany), consisting of single excitation and emission monochromators, a 350-W xenon lamp, and a photomultiplier (R928, Hamamatsu Deutschland GmbH, Herrsching, Germany). For fluorescence quantum yield calculations, a lamp and photomultiplier were calibrated for their spectral sensitivity.[35] The quantum yields obtained are based on indocyanine green (ICG) in DMSO (ϕ=0.13) as standard.[37]

2.3 *Animals, Probe Injection, and Radioactive Experiments*

The study was performed according to the Regional Animal Research Committee (authorized by Landesamt für Arbeitsschutz, Gesundheitsschutz und technische Sicherheit Berlin). Female NMRI nude mice (20 to 25 g in body weight) were used for all experiments described. For imaging studies, animals were anesthetized by intraperitoneal injection of ketamin/rompun (2:1) at a dose of 1-ml/kg body weight. MECA-79 cyanine dye and control IgM cyanine dye conjugate were injected intravenously via the tail vein as a bolus at a dose of 25 μg per animal (1 mg/kg body weight) for the *in vivo* fluorescence imaging and *ex vivo* microscopic experiments described later. For radioactive organ distribution studies, mice were injected with 2 μCi of ^{123}I-labeled antibody (n=3 for each compound and time postinjection). Animals were sacrificed and organs were prepared at 1-, 6-, 24-, and 48-h postinjection. Radioactivity was counted by gamma scintillation, values corrected for half-life decay, and expressed as percentage of injected dose/g tissue. For microautoradiography, cryosections of 10 μm thickness of peripheral lymph nodes were prepared, fixed with acetone, and air dried. Sections were dehydrated in PBS and incubated with ^{125}I-labeled MECA-79 antibody (2 μCi) for 1 h and washed with PBS. Subsequently, sections were dipped into liquid film emulsion (Amersham Biosciences, Freiburg, Germany) under dark room conditions. Following exposure of approximately 3 days, liquid file coated sections were developed according to the suppliers protocol and examined with light microscopy.

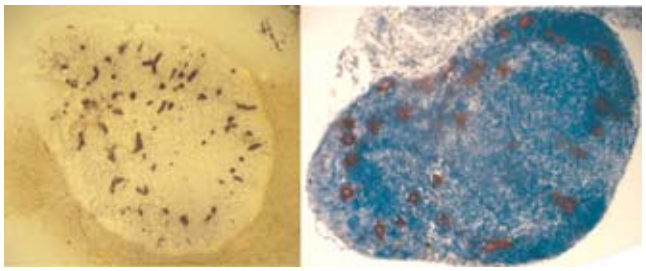

Fig. 1 Microautoradiograph showing incubation of lymph node tissue (nude mice) with ^{125}I-MECA-79 IgM. The dark spots indicating specific binding to HEVs in lymph nodes (left picture) corresponds to the binding pattern obtained by immunohistochemistry (right picture, Ref. 33).

2.4 *In-Vivo Fluorescence Imaging and Ex Vivo Macroscopic Imaging*

Fluorescence images were obtained using an imaging setup in reflection geometry. The output pulses (pulse duration: 3 ns, wavelength: 740 nm, repetition rate: 100 Hz) of an optical parametric oscillator (OPO, Coherent GmbH, Dieburg, Germany) pumped by the third harmonic (355 nm) of a Nd:YAG laser (Infinity, Coherent GmbH, Dieburg, Germany) were used to excite the dye. The laser beam was coupled into a 600-μm fiber, which was bent for mode scrambling. This fiber was placed near the objective at a defined distance from the field of view so that a circular area of about 250 mm in diameter was nearly homogeneously illuminated. Fluorescence images were recorded by employing an intensified CCD camera (Spectroscopy Instruments GmbH, Grasbrunn, Germany) equipped with optical long-pass filters to detect wavelengths between 800 and 860 nm. The cutoff at wavelengths above 860 nm is caused by a sensitivity drop of the detector. The intensifier was opened by an electrical pulse (duration 20 ns) synchronized to the laser pulse and supplied by a high voltage (HV) generator (Avtech Electrosystems Limited, Ottawa, Canada). In this way, ambient light was suppressed in fluorescence images. For detailed monitoring of dye uptake immediately after injection, 250 images were recorded in 600 s (one image in 2.4 s), followed by imaging acquisitions at 1-, 2-, 3-, 24-, and 48-h postinjection.

Lymph node tissues and cryosections (20-μm slices) were prepared from animals that were sacrificed 24 min after injection of MECA-79 cyanine dye conjugate. Highly magnified

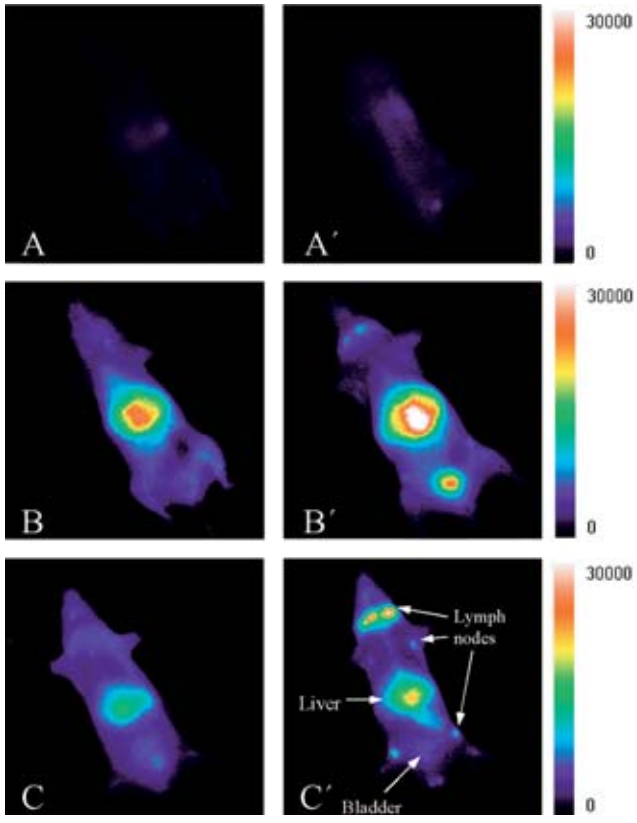

Fig. 4 Fluorescence images of mice taken before (A,A′) and after administration of 25 μg (1 mg/kg body weight) of MECA-79 (A′-C′) and control conjugate (A-C) at 10 min (B,B′) and 24 h (C,C′) after injection, respectively. Fluorescence intensities are given in a false color scale, i.e., red-white regions indicate high fluorescence. All images are normalized to the same scale as indicated at the right side.

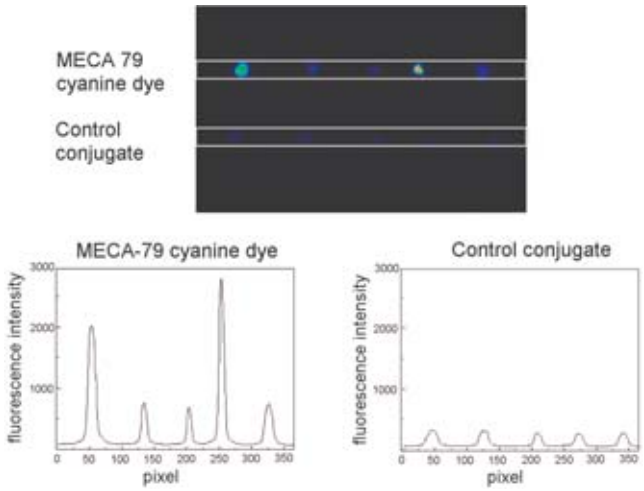

Fig. 6 Comparison of lymph nodes taken from two animals 24 h after application of contrast agents (left to right: cervical, axilliary, mesenterial, inguinal, and popliteal lymph node). The cross sections indicate fluorescence intensities scaled identically for both contrast agents. The cervical and popliteal nodes show the highest fluorescence intensity.

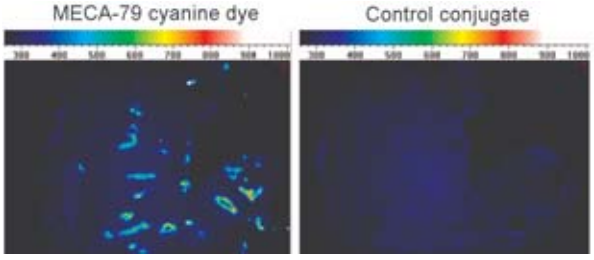

Fig. 7 Macroimages of 20-μm-thick tissue slices of a cervical lymph node. 24 h after injection of MECA-79 cyanine dye and control conjugate, respectively, mice were sacrificed and cryosections of lymph node tissue were prepared. The field of view corresponds to about 10 mm.

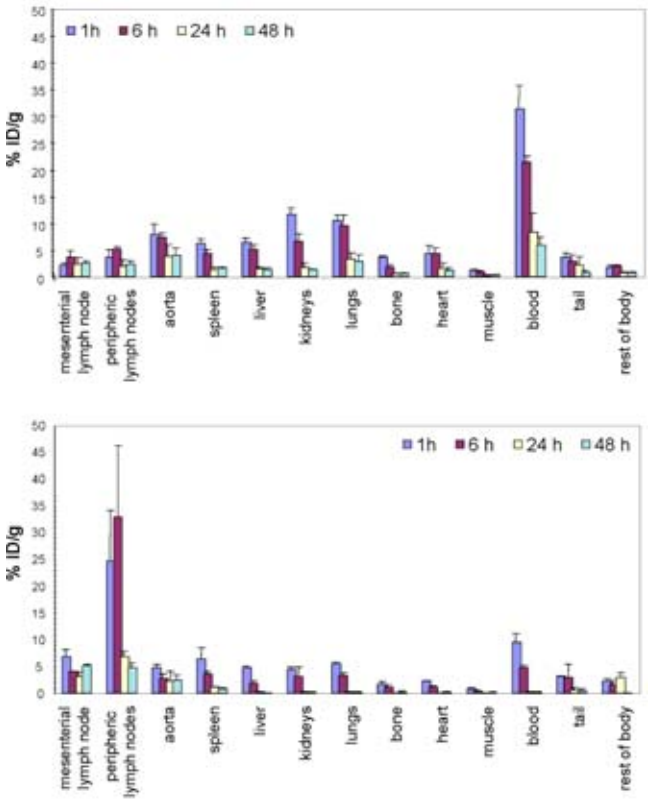

Fig. 2 Organ distribution of ^{123}I-IgM control antibody (upper chart) and ^{123}I-MECA-79 (lower chart) in NMRI nude mice depicted as percentage of injected dose per gram of respective tissue.

images of tissue sections were taken with the setup described earlier using intermediate rings and a macrolens.

3 Results and Discussion

3.1 *Radio-Iodination, Organ Distribution Studies, and Microautoradiography*

The ability of MECA-79 to act as a target-specific vehicle *in vivo* was evaluated first by radiodiagnostic techniques. For this purpose, MECA-79 was radio-iodiniated with sodium iodide (^{125}I) using a standard method. The resulting product was subjected to a simple test to prove its target binding properties by incubating cryosections, which were prepared from peripheric lymph nodes of mice, with ^{125}I-MECA-79. A microautoradiographic analysis after fixation with a photoemulsion showed the typical pattern of HEVs in peripheral lymph nodes (Fig. 1), which corresponds to the immunohistochemical appearance already published (Ref. 33). Hence, MECA-79 is capable of binding to its target and is expected to accumulate at the target site after intravenous injection into animals.

We furthermore studied the pharmacokinetic behavior of MECA-79 and quantified its organ concentrations in mice in comparison to an isotype control antibody of identical molecular weight (R4-22), both radio-iodinated with ^{123}I. The results depicted in Fig. 2 clearly show a specific uptake in lymph nodes for ^{123}I-MECA-79, whereas the isotype control remains in the blood with no considerable accumulation in lymph nodes. With respect to the uptake in other organs, both conjugates show a similar behavior, proving the exclusive expression of the target in the HEVs of lymph nodes.[32] Therefore, MECA-79 is suited as an imaging vehicle to detect glyocprotein target expression on the luminal side of HEVs, although it had to be proven that subsequent fluorescence labeling did not interfere with binding properties of the antibody.

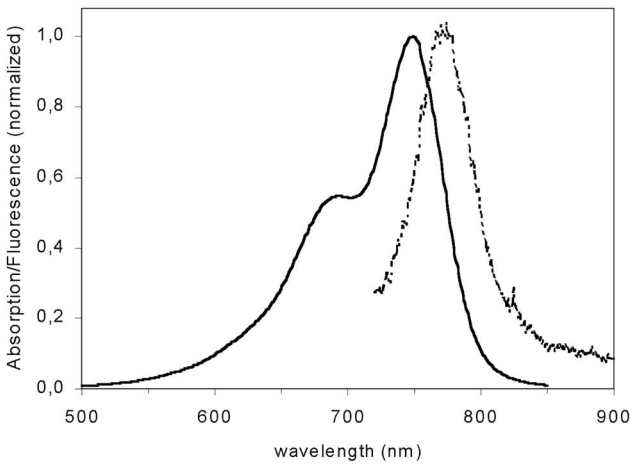

Fig. 3 Normalized absorption (solid line) and fluorescence spectra (dotted line) of MECA-79 cyanine dye conjugate. The spectra for the control conjugate look almost identical and are not included here.

3.2 *Synthesis and Properties of Fluorescent Conjugates*

MECA-79 could be readily conjugated with the indotricarbocyanine active ester by incubating the antibody with an excess of dye, according to standard labeling procedures. The selected cyanine dye has already been employed successfully in earlier work as a label for albumin and transferrin[35] and for the synthesis of receptor-targeted near-IR imaging probes.[34] Labeling of MECA-79 and the isotype control antibody R4-22 yielded a dye-to-protein ratio of 8 to 10 and for both resulting conjugates calculated from the absorption spectra. The absorption maxima were 750 nm for both conjugates and the fluorescence maxima 771 and 773 nm for MECA-79 and isotype control, respectively. The determination of the fluorescence quantum yields resulted in 0.13 and 0.14 for MECA-79 and isotype control, respectively, indicating that the dye molecules are not subject to fluorescence quenching and undergo a quantum yield increase [value for free dye reported with 0.088 (Ref. 35)]. As a consequence of the almost identical properties, both conjugates can be administered at the same doses. In Fig. 3, the near-IR absorption and fluorescence emission spectrum for MECA-79 dye conjugate is depicted.

3.3 *Fluorescence Imaging Studies and Ex Vivo Macroimaging of Tissue Sections*

The potential of MECA-79 cyanine dye conjugate to serve as a contrast agent for optical molecular imaging was investigated in nude mice in comparison to the nonbinding control conjugate. After intravenous injection of the dye solutions, the resulting contrast enhancement between lymph nodes and surrounding tissue was followed by continuous acquisition of near-IR fluorescence frames with an imaging setup in reflectance geometry. Typical fluorescence images of two mice, one

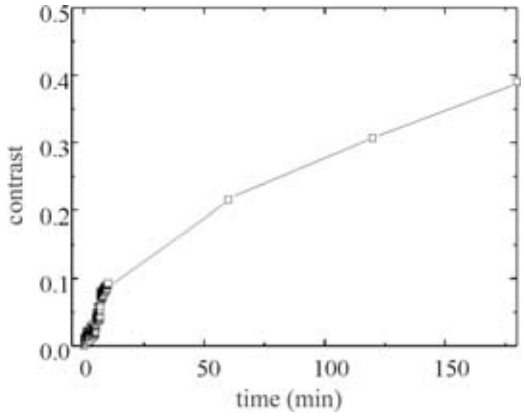

Fig. 5 Contrast (K) between lymph node region and leg muscle defined as $K=(I_{lymph}-I_{muscle})/I_{muscle}$ with time after application of MECA-79 cyanine dye conjugate. No contrast $K=0$ could be observed for the isotype IgG under the same conditions (graph not shown).

injected with MECA-79 cyanine dye and the other one with isotype control conjugate, are shown in Fig. 4. Figures 4(a) and 4(b) illustrates fluorescence images prior to application of the conjugates, Figs. 4(c) and 4(d) 10 min after IV application, and Figs. 4(e) and 4(f) at 24 h, respectively. Consistent with the uptake studies performed with a radio-labeled MECA-79 antibody, a specific binding and uptake in lymph nodes was observed as early as 10 min after injection. The ability to visualize and resolve different locations of the lymph nodes increased with time. A semiquantitative measure for imaging contrasts was obtained from intensity values determined within lymph node areas relative to adjacent areas of normal tissue (muscle). In Fig. 5, contrast is given as $(I_{lymph}-I_{muscle})/I_{muscle}$ and depicted for a time frame of up to 150 min after injection, demonstrating that target binding and blood clearance continuously improves the fluorescence contrast and visibility of the lymph nodes. At 24 h after injection, maximal contrast was achieved. At that time, the fluorescence intensity of muscle, used as reference tissue, was slightly higher than the autofluorescence intensity recorded initially (data not shown). The strong fluorescence observed in the liver is consistent with the hepatobiliary elimination pathway for this kind of macromolecules. The unspecific autofluorescence can be reduced with a manganese-free diet for the animals.

The results presented illustrate that it is possible to discriminate lymph nodes as small as 1 mm^3 from normal tissue in a scattering environment. The injected dose of 25-μg antibody corresponds to a molar dose of 10 nmol of dye per kg body weight (based on a dye-to-protein ratio of 10). In comparison with doses reported in other studies,[12,14,15] an extremely high sensitivity has been achieved.

A semiquantitative analysis of the fluorescence emission intensities of removed lymph nodes was performed to obtain a better estimate on the uptake in different lymph nodes and to allow a comparison of these tissues, which is not reasonable to be done *in vivo*, as signals are distorted due to different depth locations of the target sites within the animal. The illustration in Fig. 6 demonstrates that in principle all peripheral lymph nodes prepared from animals injected with MECA-79 cyanine dye conjugate display higher fluorescence intensities. The cervical and inguinal lymph nodes exhibit the highest signal emission (approximately 3 to 5 fold) compared to other lymph nodes. Tissues obtained after control conjugate injection are all at a measurable but similar background or nonspecific fluorescence emission level, which can be attributed to a certain remaining blood content including nonbound antibody conjugate.

Target binding of MECA-79 cyanine dye was further characterized by analyzing the lymph node sections by macroimaging. In Fig. 7, a macroimage of a 20 μ-slice of a cervical lymph node generated by using a macrolens in the imaging setup described earlier is depicted. The near-IR fluorescence pattern observed reflects the typical appearance of HEVs as shown earlier by microautoradiography and immunohistochemistry (see Fig. 1). The specificity of MECA-79 cyanine dye is supported by the observation that the control conjugate does not lead to any HEV-associated fluorescence signals in the tissue sections.

In summary, MECA-79 cyanine dye conjugate leads to specific uptake in peripheral lymph nodes after intravenous injection into mice, and generates persisting fluorescence contrast. Furthermore, the conjugate was identified *ex vivo* in tissue preparations and cryosections showing specific vascular targeting in HEVs.

4 Conclusion

We demonstrate the utility of the IgM antibody MECA-79 as optical molecular imaging probe to target HEVs in lymph nodes. Lymph node imaging is possible with high sensitivity requiring as little as 0.25 nmol per animal of this novel near-IR imaging conjugate. Targeting endothelial surface-expressed molecules, such as glycoproteins involved in leukocyte homing, deviates the need of extravascular tissue penetration of the contrast agent. As similar endothelial glycoproteins are also expressed during inflammation, the approach holds promise for the *in vivo* detection of areas of chronic inflammation. Furthermore, targeting vascular expression of specific markers in other diseases might be a promising alternative to the design of penetrating fluorescent probes directed against targets located on the tumor cell or in the extracellular space.

Acknowledgment

We gratefully thank A. Knop, H. Asbahr, M. Hasbach, V. Stickel, G. Ivkic, G. Caglar, and C. Rheinländer for their excellent technical support.

References

1. M. Rudin and R. Weissleder, "Molecular imaging in drug discovery and development," *Nat. Rev. Drug Discovery* **2**, 123–131 (2003).
2. S. Achilefu, "Lighting up tumors with receptor-specific optical molecular probes," *Technol. Cancer Res. Treat.* **3**, 393–409 (2004).
3. K. Licha, "Contrast agents for optical imaging, *Top. Curr. Chem.* **222**, 1–29 (2002).
4. M. De Grand and J. V. Frangioni, "An operational near-infrared fluorescence imaging system prototype for large animal surgery," *Technol. Cancer Res. Treat.* **2**, 553–562 (2003).
5. S. R. Cherry, "*In vivo* molecular and genomic imaging: new challenges for imaging physics," *Phys. Med. Biol.* **49**, R13–48 (2004).
6. B. Thompson and E. M. Sevick-Muraca, "Near-infrared fluorescence contrast enhanced imaging with intensified charge-coupled device ho-

modyne detection: measurement precision and accuracy," *J. Biomed. Opt.* **8**(1), 111–120 (2003).
7. D. Grosenick, H. Wabnitz, K. T. Moesta, J. Mucke, M. Moller, C. Stroszczynski, J. Stossel, B. Wassermann, P. M. Schlag, and H. Rinneberg, "Concentration and oxygen saturation of haemoglobin of 50 breast tumours determined by time-domain optical mammography," *Phys. Med. Biol.* **49**, 1165–1181 (2004).
8. C. Bremer, V. Ntziachristos, and R. Weissleder, "Optical-based molecular imaging: contrast agents and potential medical applications," *Eur. Radiol.* **13**, 231–243 (2003).
9. J. Zhang, R. E. Campbell, A. Y. Ting, and R. Y. Tsien, "Creating new fluorescent probes for cell biology," *Nat. Rev. Mol. Cell Biol.* **12**, 906–918 (2002).
10. M. D. Kennedy, K. N. Jallad, D. H. Thompson, D. Ben-Amotz, and P. S. Low, "Optical imaging of metastatic tumors using a folate-targeted fluorescent probe," *J. Biomed. Opt.* **8**(4), 636–641 (2003).
11. A. Zaheer, R. E. Lenkinski, A. Mahmood, A. G. Jones, L. C. Cantley, and J. V. Frangioni, "*In vivo* near-infrared fluorescence imaging of osteoblastic activity," *Nat. Biotechnol.* **19**, 1148–1154 (2001).
12. A. Becker, C. Hessenius, K. Licha, B. Ebert, U. Sukowski, W. Semmler, B. Wiedenmann, and C. Grötzinger, "Receptor-targeted optical imaging of tumors with near-infrared fluorescent ligands," *Nat. Biotechnol.* **19**, 327–331 (2001).
13. J. E. Bugaj, S. Achilefu, R. B. Dorshow, and R. Rajagopalan, "Novel fluorescent contrast agents for optical imaging of *in vivo* tumors based on a receptor-targeted dye-peptide conjugate platform," *J. Biomed. Opt.* **6**, 122–133 (2001).
14. B. Ballou, G. W. Fisher, A. S. Waggoner, D. L. Farkas, J. M. Reiland, R. Jaffe, R. B. Mujumdar, S. R. Mujumdar, and T. R. Hakala, "Tumor labeling *in vivo* using cyanine-conjugated monoclonal antibodies," *Cancer Immunol. Immunother* **41**, 257–263 (1995).
15. D. Neri, B. Carnemolla, A. Nissim, A. Leprini, G. Querze, E. Balza, A. Pini, L. Tarli, C. Halin, P. Neri, L. Zardi, and G. Winter, "Targeting by affinity-matured recombinant antibody fragments of an angiogenesis associated fibronectin isoform," *Nat. Biotechnol.* **15**, 1271–1275 (1997).
16. E. A. Schellenberger, A. Bogdanov, Jr., A. Petrovsky, V. Ntziachristos, R. Weissleder, and L. Josephson, "Optical imaging of apoptosis as a biomarker of tumor response to chemotherapy," *Neoplasia* **5**, 187–192 (2003).
17. R. Weissleder, C. H. Tung, U. Mahmood, and A. Bogdanov, Jr., "*In vivo* imaging of tumors with protease-activated near-infrared fluorescent probes," *Nat. Biotechnol.* **17**, 375–378 (1999).
18. M. Funovics, R. Weissleder, and C. H. Tung, "Protease sensors for bioimaging," *Anal. Bioanal. Chem.* **377**, 956–963 (2003).
19. J. M. McGreevy, M. J. Cannon, and C. B. Grissom, "Minimally invasive lymphatic mapping using fluorescently labeled vitamin B12," *J. Surg. Res.* **111**, 38–44 (2003).
20. P. Wunderbaldinger, K. Turetschek, and C. Bremer, "Near-infrared fluorescence imaging of lymph nodes using a new enzyme sensing activatable macromolecular optical probe," *Eur. Radiol.* **13**, 2206–2211 (2003).
21. E. G. Soltesz, S. Kim, R. G. Laurence, A. M. DeGrand, C. P. Parungo, D. M. Dor, L. H. Cohn, M. G. Bawendi, J. V. Frangioni, and T. Mihaljevic, "Intraoperative sentinel lymph node mapping of the lung using near-infrared fluorescent quantum dots," *Ann. Thorac. Surg.* **79**, 269–277 (2005).
22. C. P. Parungo, S. Ohnishi, A. M. De Grand, R. G. Laurence, E. G. Soltesz, Y. L. Colson, P. M. Kang, T. Mihaljevic, L. H. Cohn, and J. V. Frangioni, "*In vivo* optical imaging of pleural space drainage to lymph nodes of prognostic significance," *Ann. Surg. Oncol.* **11**, 1085–1092 (2004).
23. X. Michalet, F. F. Pinaud, L. A. Bentolila, J. M. Tsay, S. Doose, J. J. Li, G. Sundaresa, A. M. Wu, S. S. Gambhir, and S. Weiss, "Quantum dots for live cells, *in vivo* imaging, and diagnostics," *Science* **307**, 538–544 (2004).
24. T. M. Tuttle, "Technical advances in sentinel lymph node biopsy for breast cancer," *Am. Surg.* **70**, 407–413 (2004).
25. O. E. Nieweg, S. H. Estourgie, M. C. van Rijk, and B. B. Kroon, "Rationale for superficial injection techniques in lymphatic mapping in breast cancer patients," *J. Surg. Oncol.* **87**, 153–156 (2004).
26. K. T. Moesta, B. Ebert, T. Handke, D. Nolte, C. Nowak, W. E. Haensch, R. K. Pandey, T. J. Dougherty, H. Rinneberg, and P. M. Schlag, "Protoporphyrin IX occurs naturally in colorectal cancers and their metastases," *Cancer Res.* **61**, 991–999 (2001).
27. G. S. Kansas, "Selectins and their ligands: current concepts and controversies," *Blood* **88**, 3259–3287 (1996).
28. A. van Zante and S. D. Rosen, "Sulfated endothelial ligands for L-selectin in lymphocyte homing and inflammation," *Biochem. Soc. Trans.* **31**, 313–317 (2003).
29. A. Varki, "Selectin ligands," *Proc. Natl. Acad. Sci. U.S.A.* **91**, 7390–7397 (1994).
30. T. K. Kishimoto, M. A. Jutila, and E. C. Butcher, "Identification of a human peripheral lymph node homing receptor: a rapidly down-regulated adhesion molecule," *Proc. Natl. Acad. Sci. U.S.A.* **87**, 2244–2248 (1990).
31. P. R. Streeter, B. T. Rouse, and E. C. Butcher, "Immunohistologic and functional characterization of a vascular addressin involved in lymphocyte homing into peripheral lymph nodes," *J. Cell Biol.* **107**, 1853–1862 (1988).
32. C. M'Rini, G. Cheng, G. C. Schweitzer, L. L. Cavanagh, R. T. Palframan, T. R. Mempel, R. A. Warnock, J. B. Lowe, E. J. Quackenbush, and U. H. von Andrian, "A novel endothelial L-selectin ligand activity in lymph node medulla that is regulated by alpha(1,3)-fucosyltransferase-IV," *J. Exp. Med.* **198**, 1301–1312 (2003).
33. P. Hauff, M. Reinhardt, A. Briel, N. Debus, and M. Schirner, "Molecular targeting of lymph nodes with L-selectin ligand-specific US contrast agent: a feasibility study in mice and dogs," *Radiology* **231**, 667–673 (2004).
34. K. Licha, A. Becker, C. Hessenius, M. Bauer, S. Wisniewski, P. Henklein, B. Wiedenmann, and W. Semmler, "Synthesis, characterization and biological properties of cyanine-labeled somatostatin analogues as receptor-targeted fluorescent probes," *Bioconjugate Chem.* **12**, 44–50 (2001).
35. A. Becker, B. Riefke, B. Ebert, U. Sukowski, H. Rinneberg, W. Semmler, and K. Licha, "Macromolecular contrast agents for optical imaging of tumors: comparison of indotricarbocyanine-labeled human serum albumin and transferrin," *Photochem. Photobiol.* **72**, 234–241 (2000).
36. G. S. Bailey, "Labeling of peptides and proteins by radioiodination," *Methods Mol. Biol.* **32**, 441–448 (1994).
37. R. C. Benson and H. A. Kues, "Absorption and fluorescence properties of cyanine dyes," *J. Chem. Eng. Data* **22**, 379–383 (1977).